frontiers | Frontiers in Chemical Engineering

TYPE Original Research
PUBLISHED 16 July 2024
DOI 10.3389/fceng.2024.1434131

OPEN ACCESS

EDITED BY
Volker Hessel,
University of Adelaide, Australia

REVIEWED BY
Rong Tan,
Hunan Normal University, China
Chenguang Zhang,
Sanofi Genzyme, United States

*CORRESPONDENCE
Rok Ambrožič,
rok.ambrozic@fkkt.uni-lj.si

RECEIVED 17 May 2024
ACCEPTED 26 June 2024
PUBLISHED 16 July 2024

CITATION
Ramšak A, Gazvoda M, Plazl I and Ambrožič R (2024), Cu-alginate hydrogels in microfluidic systems: a sustainable catalytic approach for click chemistry.
Front. Chem. Eng. 6:1434131.
doi: 10.3389/fceng.2024.1434131

Cu-alginate hydrogels in microfluidic systems: a sustainable catalytic approach for click chemistry

Arijana Ramšak, Martin Gazvoda, Igor Plazl and Rok Ambrožič*

University of Ljubljana, Faculty of Chemistry and Chemical Technology, Ljubljana, Slovenia

This work explores the innovative use of copper-alginate (Cu-alginate) hydrogels within microfluidic systems to catalyze dipolar cycloaddition reactions, emphasizing green chemistry principles and process intensification. Utilizing naturally occurring biopolymers, such as alginates, provides an environmentally friendly alternative to conventional catalyst supports due to their biocompatibility, biodegradability, and effective metal ion immobilization capabilities. The integration of these biopolymer-based catalysts into microfluidic devices allows for precise control over reaction conditions, leading to enhanced reaction kinetics and mass transfer efficiencies. Our results demonstrate that Cu-alginate hydrogels effectively catalyze the formation of 1,4-disubstituted 1,2,3-triazoles through [3 + 2] dipolar cycloaddition reactions with high regioselectivity and conversion. The microfluidic setup ensures rapid and efficient synthesis, surpassing traditional batch reaction methods in both reaction rate and environmental impact by reducing solvent usage and waste generation. Furthermore, the use of microfluidics contributes to the reproducibility and scalability of the synthesis process, important for industrial applications. The model-based design and its simulations have been employed to further understand and optimize the reaction system. Diffusion through the gel layer and catalytic reaction kinetics estimated from experimental data were included in the model, providing a theoretical foundation for a comprehensive process evaluation. This study not only advances the field of sustainable catalysis by demonstrating the practical utility of biopolymer-supported catalysts in microfluidic systems, but also sets the stage for further research into biopolymer applications in complex chemical syntheses.

KEYWORDS

copper-alginate hydrogels, microfluidic systems, green chemistry, copper-catalyzed azide-alkyne cycloaddition (CuAAC), model-based design, click chemistry

1 Introduction

The field of green chemistry has witnessed significant progress in recent years, with an increasing emphasis on environmentally friendly and sustainable resources and processes (Jiménez-González et al., 2011). A key aspect of this shift involves the development of heterogeneous catalysts for fine chemical synthesis that also enable efficient product separation with minimal catalyst usage (Masuda et al., 2018; De et al., 2020; Sun et al., 2021). Traditionally, these catalysts have been supported on inorganic materials (Ghosh et al., 2020; Shiri and Aboonajmi, 2020; Aflak et al., 2022) or synthetic polymers (Dhital

et al., 2012; Zhang et al., 2012), but there is growing interest in the use of naturally occurring biopolymers (El Kadib, 2015; Dohendou et al., 2021) as these are abundant and renewable. Biopolymers represent a sustainable alternative and offer the dual advantage of environmental compatibility and versatile chemical properties that can be tailored to specific catalytic requirements.

Among others, alginates derived from brown algae, emerge as a promising class of biopolymers (Ambrozic and Plazl, 2021; Roquero et al., 2022; Ambrozic et al., 2024), with high sorption capacities and the ability to form various structures, including flakes, gel beads and membranes. Their versatile nature makes them ideal candidates for the immobilization of metal ions (Roquero et al., 2022) and exploring their use in catalysis (Xia et al., 2019; Wang et al., 2020). Alginates, particularly in the form of gel beads, have proven to be effective catalyst supports (Dong et al., 2011; Balakrishnan et al., 2024) due to their ability to effectively capture metal ions. Copper-alginate catalysts, for instance, have demonstrated remarkable performance in facilitating organic transformations, especially in aqueous media (Bahsis et al., 2020; Aflak et al., 2022). The complexation of copper ions with alginate ensures robust catalysis while simplifying the recovery and recycling of the catalyst.

In the realm of organic synthesis, the copper-catalyzed azide-alkyne cycloaddition (CuAAC) has emerged as a pivotal reaction that enables the formation of 1,2,3-triazoles with high regioselectivity (Reddy et al., 2007; Bahsis et al., 2018; Ben El Ayouchia et al., 2019; Bahsis et al., 2020). These triazoles are invaluable in pharmaceutical research and serve as basic structures for drug discovery and development. Copper-alginate catalysts (Reddy et al., 2007; Bahsis et al., 2020) have shown the potential to catalyze such click reactions with efficiency and precision, highlighting their utility in modern synthesis methods. The unique properties of alginates, such as their biocompatibility, biodegradability and high affinity for metal ions, make them an excellent choice for the development of reusable catalysts for click chemistry reactions.

Furthermore, the oxidative coupling of phenols and naphthols is another critical reaction that benefits from the use of copper-alginate catalysts (Reddy et al., 2007; Wu and Kozlowski, 2022). These catalysts not only improve the efficiency of such conversions, but also embody the principles of green chemistry by minimizing waste and facilitating the reuse of catalysts. The ability of alginate to form superporous hydrogels further enhances its utility by providing a large surface area for catalytic reactions and ensuring efficient interaction between the catalyst and substrates. These advances reflect a broader trend in catalysis research towards more sustainable and recyclable catalyst systems. The immobilization of copper on biodegradable supports such as alginate enables efficient catalysis while simplifying the recovery and reuse of the catalyst.

Nevertheless, in many batch systems, mass transfer limitations remain the biggest drawback to effective conversion. Therefore, the transition from batch to continuous process operation has been recognized as a key factor in achieving green chemistry goals (Jiménez-González et al., 2011; Newman and Jensen, 2013; Tamborini et al., 2018). In line with that, microfluidics has emerged as a revolutionary approach in the field of chemical engineering and catalysis (Goy et al., 2019; Ambrozic et al., 2024; Menegatti et al., 2024), offering unprecedented control over reaction conditions and enabling process intensification. The unique properties of microfluidic devices, such as the large surface-to-volume ratio and precise control of flow dynamics, allow for improved mass and heat transfer, resulting in higher reaction rates and improved product yields (Wohlgemuth et al., 2015). For heterogeneous catalysts, such as copper-alginate, microfluidics provides a platform for fine-tuning reaction parameters and achieving optimal catalytic performance (Milozic et al., 2018; Vicente et al., 2020; Ambrozic et al., 2024). This technology also enables the integration of multi-step processes in a single device (Pohar et al., 2012), significantly reducing the time and resources required for complex syntheses. By leveraging the precision and scalability of microfluidics, researchers can achieve process intensification that maximizes the efficiency of copper-alginate-catalyzed conversions.

Therefore, combining microfluidics with stimuli-responsive smart materials, such as electro-responsive copper-alginate (Nie et al., 2018; Goy et al., 2019; Menegatti et al., 2024), presents an interesting route for *in situ* catalyst deposition and regeneration. These smart materials can undergo reversible changes in their structure and functionality in response to external stimuli such as electric fields (Ambrozic et al., 2024), allowing precise manipulation of the catalyst within microfluidic channels. This approach not only facilitates the deposition of copper-alginate in specific regions of the microreactor, but also enables real-time adjustments to the catalyst's properties, providing greater control over the reaction environment. The integration of microfluidics with stimuli-responsive materials (Kang et al., 2013; Huang et al., 2020) opens up new possibilities for the development of advanced catalytic systems that can adapt to changing conditions, ensuring optimal performance for diverse chemical processes.

In this context, the present work seeks to explore the efficacy of copper-alginate catalysts for 1,3-dipolar cycloaddition reactions. The use of such catalysts represents a significant step forward in the development of environmentally friendly and cost-effective methods for organic synthesis. Preliminary results demonstrate that this catalyst system exhibits excellent activity and selectivity towards the formation of triazoles, with the microfluidic environment facilitating rapid and efficient mass transfer and reaction kinetics. The electrodeposition process allows precise control of hydrogel formation, enabling the tuning of the catalytic properties by adjusting the copper content and gel morphology. The reusability of the catalyst, a crucial aspect of sustainable chemical processes, is also being investigated, highlighting the potential of this approach to make an important contribution to the field of green catalysis. By integrating Cu-alginate hydrogels into microfluidic systems, we present a scalable, environmentally friendly and highly effective strategy for conducting dipolar cycloadditions. This work not only opens up new avenues for the use of biopolymer-supported catalysts in organic synthesis, but also demonstrates the immense potential of microfluidic devices to improve the sustainability and efficiency of chemical processes.

2 Experimental

2.1 Materials

Alginic acid sodium salt from brown algae (medium viscosity, ≥2.000 cP, further marked as alginate, 96%), copper

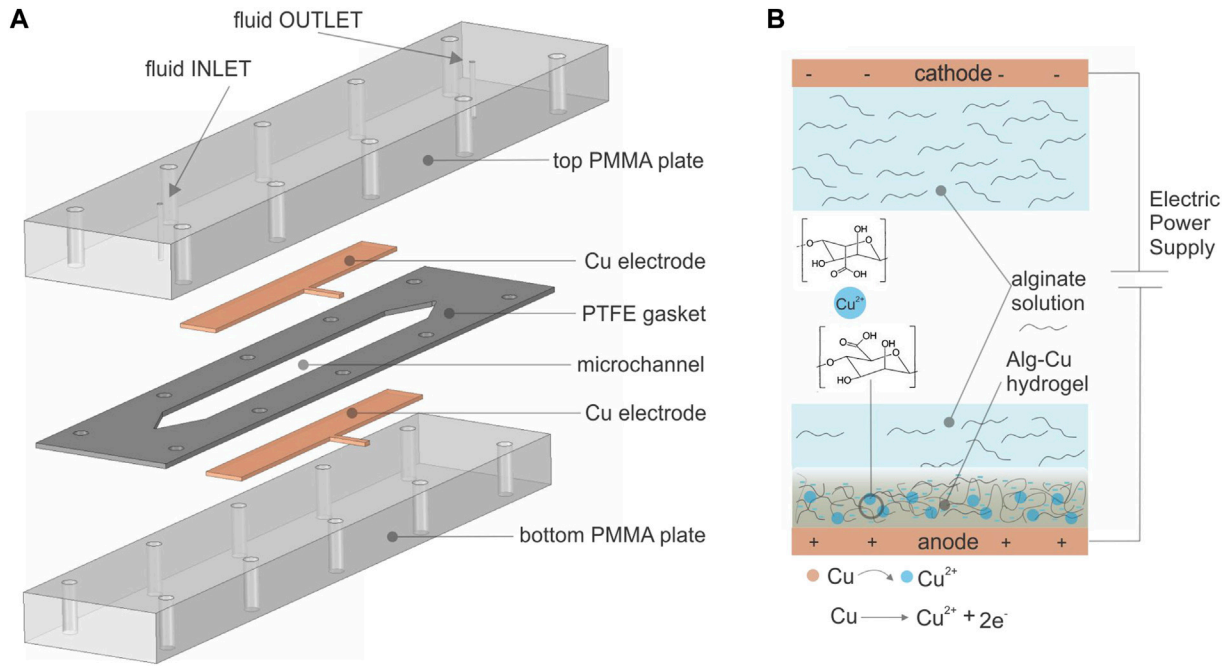

FIGURE 1
A custom-made transparent microfluidic system with integrated copper (Cu) plate electrodes, placed between PMMA layers separated by a PTFE sealing film that formed the shape of a channel **(A)**. The schematic representation of the mechanism of formation Alg-Cu hydrogel on anode surface by electrodeposition method **(B)**.

standard solution ($Cu(NO_3)_2$ in HNO_3 0.5 mol/L), ethylenediaminetetraacetic acid disodium salt (EDTA), sodium sulfate (anhydrous, 99%), hydrochloric acid, acetic acid, N-(2-Hydroxyethyl)piperazine-N′-(2-ethanesulfonic acid) (≥99.5%, HEPES), citric acid, ethanol, and ethyl acetate were used as received from Merck KGaA (Darmstadt, Germany). Phenylacetylene (further abbreviated as PA) was purchased from Sigma Aldrich and benzyl azide (further abbreviated as BA) was synthesized according to the literature procedure (Zhang et al., 2020). All experiments were carried out in ultrapure water (18.2 MΩ cm).

2.2 Design of microfluidic device

Electrochemical experiments were conducted in a custom-made transparent microfluidic system (Figure 1) with plate-plate geometry. The system featured patterned copper (Cu) plate electrodes purchased from commercial suppliers. The two electrodes were integrated between 10 mm thick poly (methyl methacrylate) (PMMA) layers serving as housings and were separated by a 1,000 μm thick polytetrafluoroethylene (PTFE) gasket/spacer that defined the geometry of the microchannels. To prevent leakage, all layers were placed on top of each other and fastened with screws. The microfluidic channel had a width of 10 mm, a height of 1,000 μm and a length of 100 mm, with an active electrode area of 10 mm × 100 mm. Compared to conventional electro-micro devices, where the electrodes are attached to the side walls, the electrodes at the bottom/top of the microfluidic channel allow for a larger electrode area, resulting in more efficient hydrogel formation and more applicable molecular diffusion.

2.3 Preparation of alginate copper catalyst (Alg-Cu)

Alginate hydrogel films were prepared using a previously described electrochemical deposition method (Ambrozic and Plazl, 2021). Briefly, sodium alginate (1.0% w/v) was dissolved in a 100 mM Na_2SO_4 aqueous solution, stirred overnight, and then filtered with a 40 μm porous glass filter to remove undissolved impurities. Before each experiment, the pH of the solution was adjusted to 6.0 with 1M HCl or 1M NaOH. Prior to electrodeposition, the microfluidic channel was immersed with alginate solution to ensure that the microchannel was completely filled. The flow of solution (200 μL/min unless otherwise specified) was controlled by a programmable syringe pump (PHD 4400 Syringe Pump) with a stainless-steel syringe (Harvard Apparatus, Holliston, MA). An alligator clip was used to connect the plate electrodes to a DC power supply (2,400 Sourcemeter, Keithley). The parallel Cu plate electrodes served as both cathode (negatively biased electrode) and anode (positively biased electrode). Prior to the experiments, the electrodes were successively cleaned with acetone, ethanol and water under sonication for 5 min each. Electrodeposition was performed at a constant current density (3.5 A/m^2) over a specific period of time (120 min, unless otherwise specified) with typical voltages of 2–3 V. During electrodeposition, the copper on the anode surface is oxidized to Cu^{2+}, which triggers the formation of copper-alginate hydrogel

(further abbreviated as Alg-Cu) on the anode surface. After each deposition step, the electrode was disconnected from the power supply and the microchannel was rinsed several times with alginate-free aqueous Na_2SO_4 solution and finally with pure water to remove unbound molecules. So fabricated electrode (coated with Alg-Cu hydrogel) was left in the microdevice housing and stored in aqueous medium at room temperature for further use. To determine the total amount of Cu ions cross-linked in the hydrogel, the hydrogel films were dissolved in EDTA (10 mM) and analyzed by AAS.

The electrodeposition process of alginate hydrogel was simulated by computational fluid dynamics (CFD) simulations using Ansys FLUENT 2022 R2. The detailed structure of the model is presented in our earlier study (Ambrozic et al., 2024), with important information provided in Supplementary Material. The first step in the construction of the CFD model was the design of the microchannel geometry and its meshing. Subsequently, the distribution of the electrical potential throughout the microchannel was simulated, considering the experimental conditions (2 V) at a specific current density (1–5 A/m^2). The obtained concentration profiles were correlated with the experimentally determined hydrogel thickness at specified time interval, which allowed the estimation of the kinetic parameters of the redox reaction and especially gel formation. The estimated values were then used for all further simulations and predictions, providing a comprehensive approach to understanding the complex processes occurring within the microfluidic system, which is crucial for optimizing the process conditions.

2.4 Alg-Cu hydrogel characterization

The hydrogels morphology was analyzed by field emission scanning electron microscopy (SEM). For this purpose, electrodeposition was performed at constant current density (1, 2, 3.5 and 5 A/m^2) for a specific period of time (30, 60 and 120 min) with typical voltages of 2–3 V. Prior to the measurements, all samples were freeze-dried in liquid nitrogen and coated with gold sputter. Scratch analysis and the thickness of the hydrogel films were analyzed using a high-speed optical microscope (Motion Scope) and a thickness gage (Mitutoyo Absolute Digimatic Height Gage), respectively.

Chemical analysis of the hydrogel films was performed by Fourier transform infrared spectroscopy (IR spectrometer Spectrum BX FTIR Perkin-Elmer) in the wavelength range 4,000–500 cm^{-1}.

The copper concentration was determined by atomic absorption spectrometry (AAS). First, Cu calibration curve (Supplementary Figure S1) was constructed to determine the concentration-absorbance relationship required for the quantitative determinations. Calibration curves with at least five points within the expected concentration range were constructed for all experiments.

2.5 Synthesis of 1-benzyl-4-phenyl-1H-1,2,3-triazole in microfluidic device

Benzyl azide (160 mg, 1.2 mmol) and phenylacetylene (102 mg, 1.0 mmol) were mixed with a solution of water and ethanol (1:1) (20 mL) to obtain a homogeneous, stable white emulsion. The mixture was filled into a stainless-steel syringe, inserted into pump (PHD 4400 Syringe Pump) and connected to the microfluidic device by suitable fittings. The flow rate of the solution was adjusted to the desired value (5–20 μL/min) and the reaction was initiated by simultaneously contacting the reactant mixture with the catalytic sites of the Alg-Cu hydrogel. Note that the Alg-Cu hydrogel was formed in the previous step (120 min at 3.5 A/m^2). All experiments were performed at room temperature and the eluate was collected in the microfluidic outlet. The triazole product was extracted from the resulting mixture with ethyl acetate (3 × 50 mL). The combined organic phases were dried over sodium sulphate and the solvent was removed under reduced pressure to give the pure 1-benzyl-4-phenyl-1*H*-1,2,3-triazole product. ^{1}H NMR of 1-benzyl-4-phenyl-1*H*-1,2,3-triazole ($CDCl_3$, 500 MHz): δ 7.81–7.78 (m, 2H), 7.66 (s, 1H), 7.42–7.30 (m, 8H), 5.58 (s, 2H). Spectroscopic data are in agreement with the literature (Alonso, Moglie, Radivoy and Yus, 2010).

Additionally, the conversion into to the 1-benzyl-4-phenyl-1*H*-1,2,3-triazole product was determined from ^{1}H NMR by using 1,3,5-trimethoxybenzene as an internal standard. Namely, the conversion into the product was determined by comparing the integrals of the characteristic resonances of 1-benzyl-4-phenyl-1*H*-1,2,3-triazole product, i.e., δ 7.81–7.78 ppm (m, 2H), 7.66 ppm (s, 1H), 5.58 ppm (s, 2H), with the integrals of the resonances of an internal standard 1,3,5-trimethoxybenzene, i.e., δ 6.10 ppm (s, 3H) and 3.77 ppm (s, 9H). The conversions into 1-benzyl-4-phenyl-1*H*-1,2,3-triazole of 120 min, 60 min flow reactions were determined to be 99% and 55%, respectively (see Supplementary Figures S2, S3 for NMR spectra).

2.6 Synthesis of 1-benzyl-4-phenyl-1H-1,2,3-triazole in batch

The batch experiment was performed in a 50 mL glass baker. Initially, the Alg-Cu hydrogel was formed using a disc-shaped copper electrode system with a working area of 5 cm^2 connected to a DC power supply (2,400 Sourcemeter, Keithley). The Alg-Cu hydrogel was deposited onto the anode surface from an alginate solution (1.0% w/v alginate, 100 mM Na_2SO_4) under constant conditions (120 min at 3.5 A/m^2). Subsequently, the hydrogel was washed extensively with buffer solution. The hydrogel-coated electrode was placed in a reaction vessel to which benzyl azide (160 mg, 1.2 mmol), phenylacetylene (102 mg, 1.0 mmol) and 20 mL of water-ethanol mixture (1:1) were added. The reaction vessel was placed on a magnetic stirrer and the reaction mixture was stirred for 2 h at room temperature. After completion of the reaction, the product was filtered to remove undissolved moieties. The resulting mixture was extracted using ethyl acetate (3 × 50 mL), the combined phases were dried over sodium sulphate and the solvent was removed under reduced pressure to obtain the crude product, which was analyzed by ^{1}H NMR to determine the conversion to 1-benzyl-4-phenyl-1*H*-1,2,3-triazole as described above in Section 2.5. The conversion to 1-benzyl-4-phenyl-1*H*-1,2,3-triazole was determined to be 10% (see Supplementary Figure S4 for NMR spectra).

2.7 Model development

The aspect ratio of the microfluidic system (Figure 1) suggests that the influence of the small side surfaces on the velocity profile is negligible. This allows for the development of 2D model equations for substrates and products within the liquid and gel microreactor domains. The equations for the mass balance with suitable boundary conditions for the substrates and the product in the liquid phase with stationary unidirectional laminar flow of a Newtonian fluid are as follows:

$$-u_x(y)\frac{\partial C_{i,l}}{\partial x} + D_{i_l}\frac{\partial^2 C_{i,l}}{\partial x^2} + D_{i_l}\frac{\partial^2 C_{i,l}}{\partial y^2} = 0 \quad (1)$$

with appropriate boundary conditions:

$$C_{i,l}(0,y) = \begin{cases} C_{i,l,in};\ i = PA \\ C_{i,l,in};\ i = BA;\ hg \le y \le H; \\ 0;\quad i = P \end{cases}$$

$$\frac{\partial C_{Fi,l}}{\partial x}(L,y) = 0;\ hg \le y \le H;$$

$$\frac{\partial C_{i,l}}{\partial y}(x,0) = 0;\ 0 \le x \le L;\ -D_{i,l}\cdot L\cdot W\frac{\partial C_{i,l}}{\partial y}(x,h_g) = -D_{i,g}\cdot L\cdot W\frac{\partial C_{i,g}}{\partial y}(x,h_g);\ 0 \le x \le L; \quad (2)$$

and for substrates and product in the gel phase:

$$D_{i,g}\frac{\partial^2 C_{i,g}}{\partial x^2} + D_{i,g}\frac{\partial^2 C_{i,g}}{\partial y^2} - k_{cat}\,C_{PA,g}C_{M,g} = 0 \quad (3)$$

with boundary conditions:

$$\frac{\partial C_{i,g}}{\partial x}(0,y) = \frac{\partial C_{i,g}}{\partial x}(L,y) = 0;\ 0 \le y \le hg;$$
$$\frac{\partial C_{i,g}}{\partial y}(x,0) = 0;\ 0 \le x \le L;$$
$$C_{i,g}(x,h_g) = C_{i,l}(x,h_g);\ 0 \le x \le L; \quad (4)$$

In Equations 1–4, L [m] is the length and W [m] is the width of the microsystem between the two plates, the thickness of the single gel layer is h_g, and the height of the liquid flow is $H - h_g$ [m]. The $u_x(y)$ is the velocity profile of the aqueous laminar flow (*Poiseuille flow*). The $C_{i,l}$ (mol m^{-3}) is the concentration in the liquid phase, while $C_{i,l,in}$ is the inlet concentration, where the subscript i denotes the substrates phenylacetylene (PA), Benzyl azide (BA), and the triazole product (P). The D_{i_l} (m^2 s^{-1}) are the diffusion coefficients of both the substrates and the product in the liquid phase (the estimated values: $D_{PA_l} = 0.97\,10^{-9}$, $D_{BA_l} = 0.83\,10^{-9}$, $D_{P_l} = 0.67\,10^{-9}$), and D_{i_g} (m^2 s^{-1}) are effective diffusion coefficients of substrates and product in the gel phase with estimated values in the range 10^{-10}. The k_{cat} is the reaction rate constant for the second order catalytic reaction with an estimated value of 0.49 10^{-5} (m^3 mol^{-1}s^{-1}) at a Cu catalyst concentration of 11.22 mM.

3 Results and discussion

The innovative integration of Alg-Cu hydrogels into a microfluidic framework to catalyze the dipolar [3 + 2] cycloaddition reaction exemplified the synthesis of triazole, i.e., 1-benzyl-4-phenyl-1*H*-1,2,3-triazole, from benzyl azide and phenylacetylene. Such an approach enables process intensification through unique stimuli responsive features that combine *in situ* catalyst fabrication with model click reaction operating in continuous/flow regime. Since the Alg-Cu catalyst is the most important transformation vehicle, its detailed characterization was performed first.

3.1 *In situ* Alg-Cu formation by electrodeposition method

The first step to achieve this goal was the immobilization of copper ions in a polymeric alginate network. In doing so we employed advanced electrodeposition method coupled with a microfluidic device that enables precise deposition control. The copper electrodes were subjected to an electric potential, whereby elemental copper is oxidized on the anode surface, resulting in a controlled release of Cu^{2+} ions. The Cu^{2+} ions interact with free alginate chains from the solution, resulting in the formation of a gel layer on the anode surface. The thickness of the hydrogel can be adjusted by the electrodeposition conditions, such as current density and deposition time. As a result, the copper concentration trapped in the hydrogel network also changes and depends on both conditions. The electrodeposition experiments were conducted at a constant flow rate of the alginate solution (200 uL/min) for different time intervals (from 10 min to 120 min) and current densities (1, 2, 3.5 and 5 A/m^2). As demonstrated in our previous work, the longer the time and current density, the thicker the hydrogel. The same was observed here. The evolution of the hydrogel thickness, shown in Figure 2, was analyzed using a high-speed optical microscope. It was found that all samples showed a similar tendency, namely, rapid growth in the initial phase and then slowing down as they approached a steady state. The hydrogel thickness obtained ranged from 200 to 500 μm, depending on the current density used. It is evident that Cu oxidation and the resulting deposition process are more effective at higher electric current. Nevertheless, it is important to emphasize that the thickness and volume of the hydrogel change significantly when it is not in an aqueous medium, resulting in drying of the gel (data not shown). To ensure complete hydration of the hydrogels and prevent drying, all gels formed were stored in a microfluidic device filled with a buffer solution.

In the next step, the electrodeposition process was simulated using a CFD model. First, the distribution of the electrical potential throughout the microchannel was simulated (Figure 3A), reflecting the experimental conditions with a voltage between cathode and anode of 2 V at a current density of 3.5 A/m^2. The electrical potential gradient propagates from a positive value at the anode surface to a negative value at the cathode surface and shows a fairly symmetrical distribution over the channel height. Due to exclusion effects, the electrical potential reaches zero in the middle of the channel. Subsequently, the temporal evolution of the hydrogel growth during the deposition process was investigated. The representative concentration distributions of the hydrogel over the channel height at the beginning and at the end of the process are shown in Figure 3B. As expected, the concentration decreases with increasing distance from the anode and reaches an equilibrium state after a certain time (timestep = 100). The simulation reflects the experimental values, with the thickness of the hydrogel formed

10.3389/fceng.2024.1434131

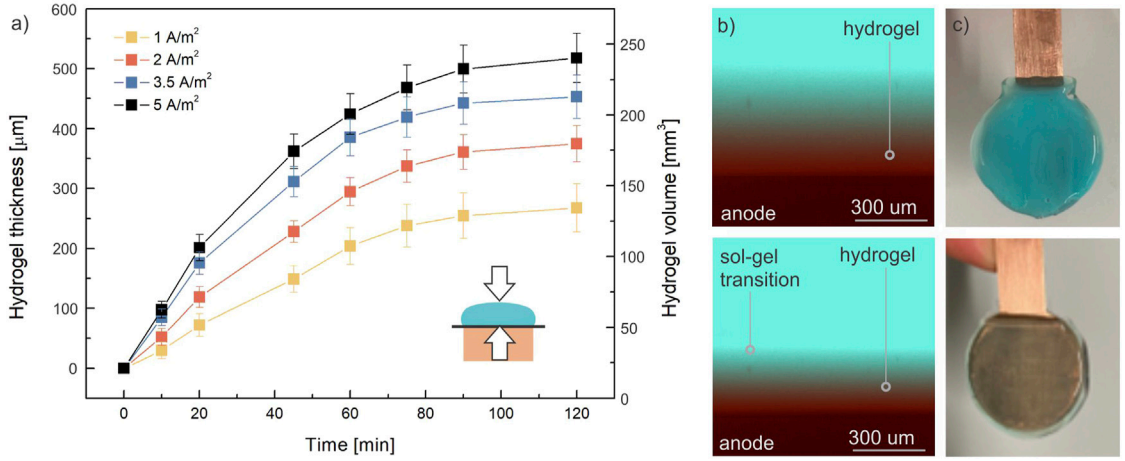

FIGURE 2
The time evolution of hydrogel thickness on an anode surface **(A)** at different current densities (1, 2, 3.5 and 5 A/m^2) and representative figure of formed hydrogel analyzed with a high-speed optical microscope **(B)**. The color of hydrogels changes from light blue to dark blue **(C)** when time and/or current density was increased. For improved resolution batch experiments are shown in figures **(C)**.

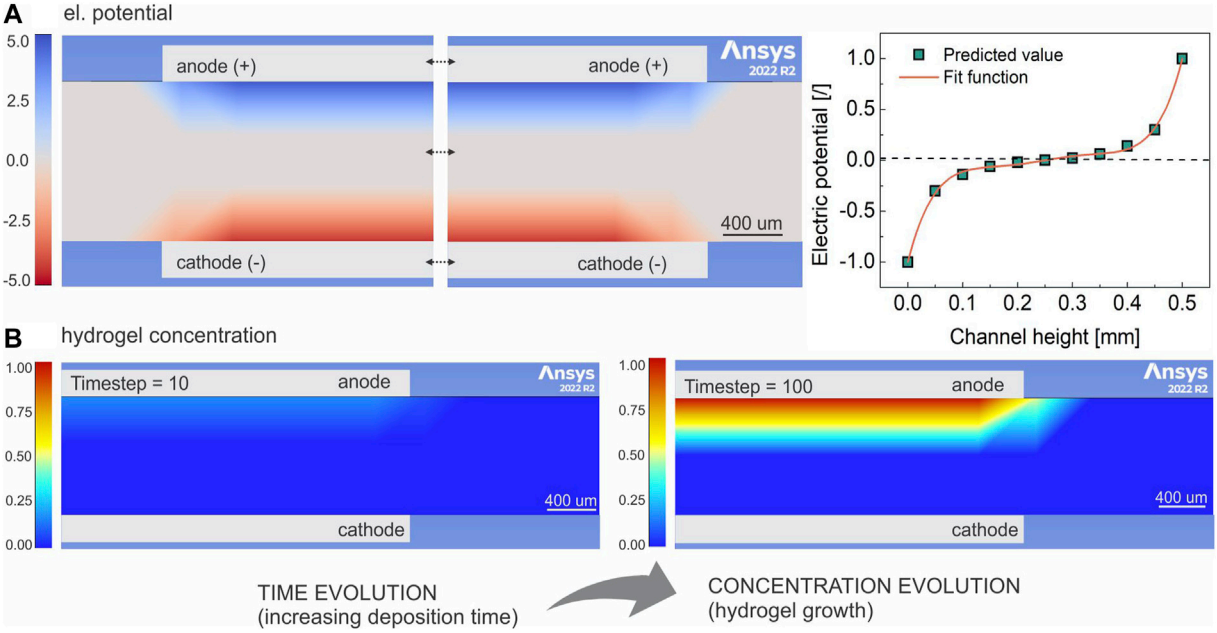

FIGURE 3
The simulation of electric potential through the microchannel height **(A)**, and evolution of the concentration profile during the electrodeposition process at various time frames of deposition process **(B)**. One timestep corresponds to approximately 1 minute in real experiments. The CFD simulations were performed using Ansys FLUENT.

approaching half the channel height. In addition, the hydrogel thicknesses at the individual deposition times (measured at the point where the hydrogel concentration still changes relative to the bulk concentration) were compared with experimentally determined values (high-speed optical microscope image–Figure 2B), allowing kinetic parameters for hydrogel growth to be determined. The reaction rate constants were then used for all subsequent steps and validated with experimental data at different current densities and deposition times. Good agreement between experiments and simulation was achieved, highlighting the utility value of the method (especially for the later stage of process development).

3.2 Characterization of the Alg-Cu hydrogels

To analyze the chemical structure and morphology of the hydrogels formed, the samples were frozen in liquid nitrogen and then lyophilized at −40°C. The FT-IR spectrum of Alg-Cu hydrogels

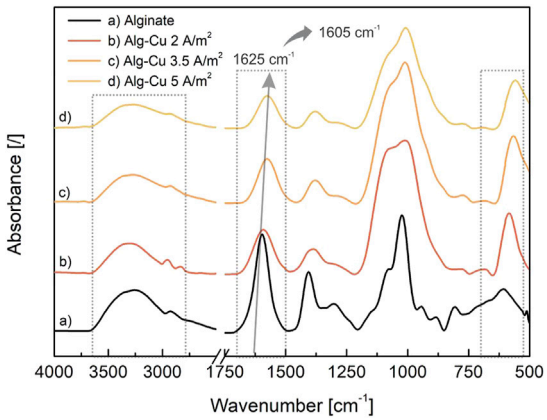

FIGURE 4
The FT-IR of neat alginate **(A)** and Alg-Cu hydrogels prepared at various current densities: 2 A/m² **(B)**, 3.5 A/m² **(C)**, and 5 A/m² **(D)**.

prepared at different current densities (2, 3.5 and 5 A/m^2) is shown in Figure 4. The IR spectrum of pure alginate is also shown for comparison. The FT-IR spectra of alginate and dried Alg-Cu hydrogels showed several peaks with the same wavenumber. Thus, characteristic peaks of carboxylate group COO- (symmetric stretching vibrations at 1,605–1,625 cm^{-1} and 1,414 cm^{-1}), hydroxyl groups (broad peak at 3,350 cm^{-1}), C-H bond (stretching vibrations at 2,930 cm^{-1} and 882 cm^{-1}) and ethers linkages C-O-C (symmetric stretching vibrations at 1,030 cm^{-1}) were observed. A similar spectrum of related products was observed elsewhere (Bahsis et al., 2020; Fraczyk et al., 2020). In addition, the Alg-Cu spectrum shows more distinct peak at 620 cm^{-1}, which is probably due to Cu-O interactions that were not present in the spectrum of sodium alginate. Furthermore, after the crosslinking process, the spectral band corresponding to the asymmetric stretching vibration of COO- shifted downward (from 1,625 cm^{-1} to 1,605 cm^{-1} for Alg and Alg-Cu, respectively). Similar was reported elsewhere (Bahsis et al., 2020). The characteristic peaks for COO- groups (1,605 cm^{-1} and 1,414 cm^{-1}) were also less pronounced compared to pure alginate, indicating their involvement in the coordination process through electrostatic interaction between the alginate chains and copper (II) ions. Copper (II) ions serve as crosslinking agents as they enable the guluronic acid units of the alginate polymers to effectively capture divalent cations. This observation confirms the successful crosslinking of the alginate polymer with copper ions. Due to the enhanced Cu-Alg interactions, the intensity of this characteristic peak of hydroxyl groups decreased with higher current density, resulting in an increased number of metal-polymer interactions. Finally, as the gelation process progressed (at higher current densities), fewer expressed peaks were observed, which is typical for more crosslinked samples. Therefore, it is hypothesized that a higher concentration of Cu^{2+} may be formed during a more intense electrodeposition process, resulting in a denser hydrogel structure. This assumption was later confirmed by AAS analysis.

To evaluate the morphology of the hydrogels, SEM analyses were performed next. The SEM images, particularly evident in Figure 5, show a highly intricate porous structure characterized by a multitude of crosslinks, which are crucial for the mechanical integrity and functionality of the hydrogels. Notably, the average diameter of the surface pores was in the range of a few nm, while the average diameter of the interconnected pores was ranging from 200 nm to a μm scale, illustrating the ultrafine nature of these structures. This variation in pore size indicates a well-organized porous network that can support diverse biological and chemical applications by facilitating varied molecular interactions.

The morphology of the hydrogel is consistent with results reported elsewhere (Baig and Varma, 2013; Bahsis et al., 2020), suggesting a common structural paradigm in hydrogel formation. SEM analysis further demonstrated that the hydrogels possess a highly permeable structure. This permeability is essential for the rapid diffusion of small molecular entities, such as benzyl azide (BA) and phenylacetylene (PA), through the gel matrix. The effective adsorption and desorption of copper ions (Cu) within these hydrogels is particularly noteworthy as they play a decisive role in the overall activity of the hydrogel/catalyst. The ability of the hydrogels to efficiently channel these metal ions through their structure without compromising their integrity or functionality underscores their potential utility as catalysts for click cycloaddition reactions.

The catalytic activity of Alg-Cu hydrogels is due to the immobilized copper species. The higher the Cu concentration, the more stable the hydrogel. In addition, higher Cu loading improves the activity of the catalyst as more active sites are available for the copper-catalyzed reaction between BA and PA molecules. Accordingly, the Cu concentration within hydrogel was examined by AAS method. The hydrogels were prepared according to the method described above with different electric current densities (1–15 A/m^2) and electrodeposition times (30–120 min). Afterwards, the hydrogels were completely dissolved in EDTA solution (100 mM), as EDTA acts as a strong chelating agent for various metallic cations, including copper. The results of the measured Cu concentrations are display in Figure 6 and demonstrates near perfect linear correlation. This is especially true for the samples prepared with different current densities. Obviously, the higher the current density, the more Cu ions are coordinated in the hydrogel. On the other hand, a certain linear trend is also observed with increasing duration of electrodeposition, although a deviation from linearity was observed at longer durations (120 min). A similar trend was observed for the thickness of formed hydrogels (Figure 2). Namely, a linear growth at shorter deposition time followed by a slower growth at longer deposition. We assume that diffusion limitation, due to gelation process, was reached at this point reducing the electric potential further away from the electrode. Nevertheless, the relationship and correlation obtained allow fine tuning of catalyst molarity and thus its activity by external electrical stimuli according to the application requirements. Needless to say, that this feature gives an enormous advantage for niche-oriented industrial-based applications and can also serve to optimise the loading of the catalyst.

3.3 Catalytic activity of Alg-Cu catalyst for click reaction, copper-catalyzed azide-alykne cycloaddition (CuAAC)

The first goal, the formation and immobilization of a stable and active Cu-based catalyst for catalytic dipolar cycloaddition reactions

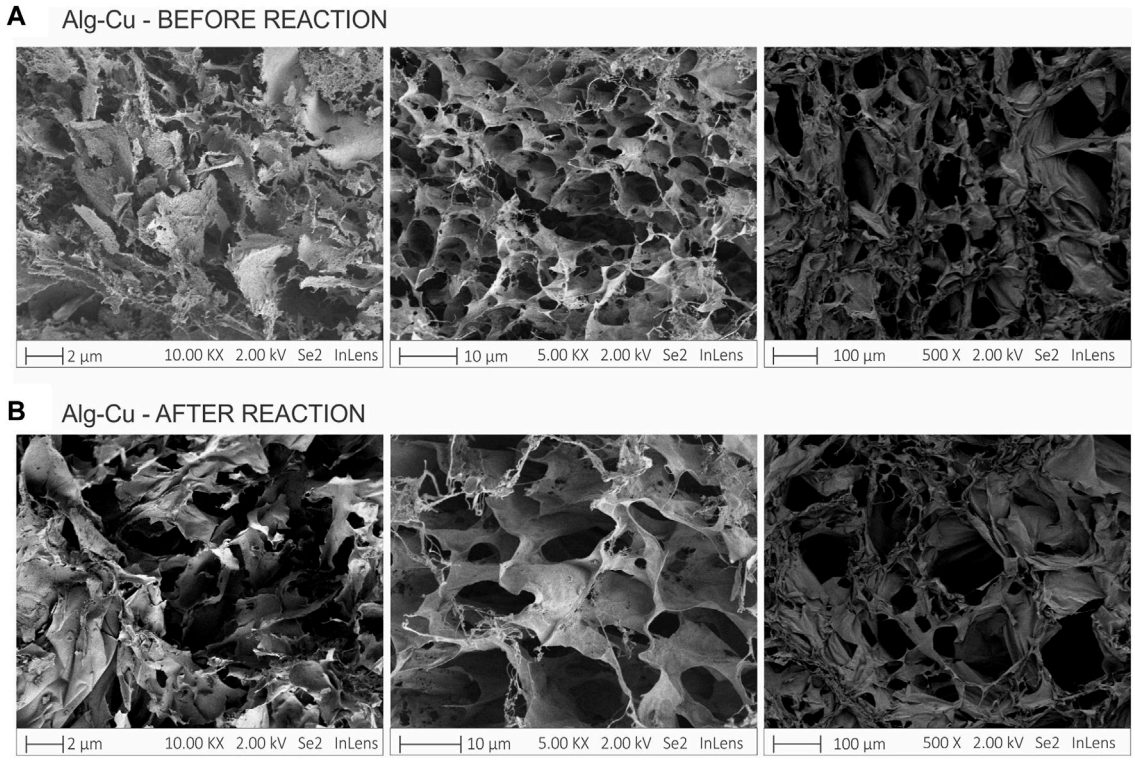

FIGURE 5
SEM images of Alg-Cu hydrogels before **(A)** and after **(B)** the copper-catalyzed azide-alykne cycloaddition (CuAAC) reaction at various resolution.

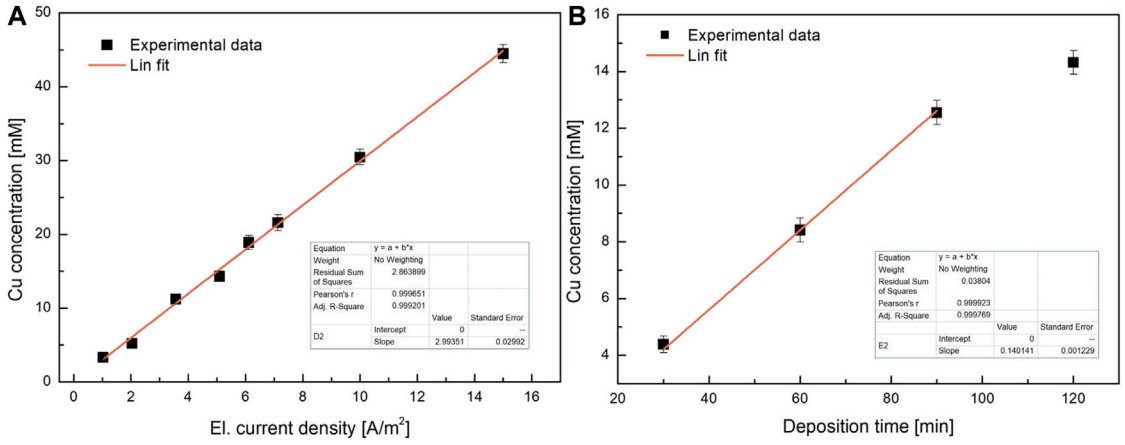

FIGURE 6
The Cu concentration as a function of current density **(A)** and deposition time **(B)** during electrodeposition process. Note that constant deposition time (120 min) was selected for experiments with varying current density, while constant current density (5 A/m^2) was selected for experiments with varying deposition time.

within a microfluidic system, was thus successfully accomplished. Naturally, the next step involved the implementation of model reaction using two commonly applied substrates for CuAAC, namely, benzyl azide and phenylacetylene (Figure 7). Initially, the Alg-Cu hydrogel was formed *in situ* within the microfluidic devices by electrodeposition process, using 3.5 A/m^2 for 120 min. The alginate solution was constantly pumped through at a flow rate of 200 uL/min. The microchannel was then washed extensively with aqueous buffer solution (100 mM Na_2SO_4) to remove all unbound alginate molecules. Finally, the mixture of BA and PA was added to a syringe pump and connected to the inlet of the microreactor. By changing the flow rate (5 and 10 µL/min), the residence time was adjusted accordingly (from 1 h to 2 h). The eluate was continuously collected at the outlet of the microfluidic device.

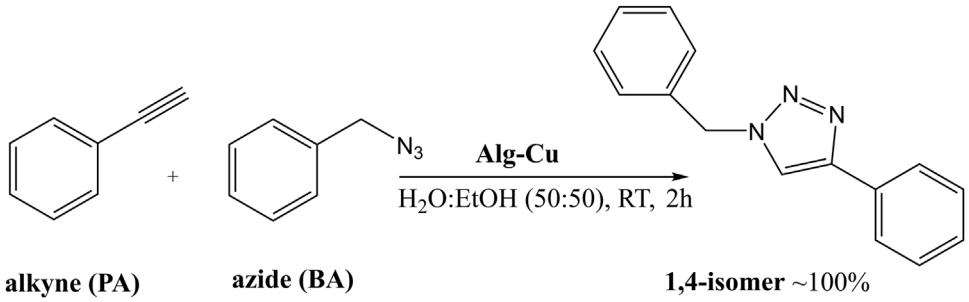

FIGURE 7
Alg-Cu based catalysed [3 + 2] cycloaddition reaction of benzyl azide and phenylacetylene.

The experiments began with the intention of transferring the model reaction from the batch to the flow system (microreactor). The use of a constant flow feed in a microfluidic device offers several advantages for mass transfer over batch operations. In continuous flow systems, reactants are continuously supplied and removed, minimizing concentration gradients and improving mass transfer efficiency. This continuous feed ensures a steady supply of reactants to the catalytic sites, maintaining high reaction rates and reducing mass transfer limitations caused by decreasing reactant concentration (as the reaction progresses). In addition, the laminar flow in the microchannels allows for well-defined conditions, which are crucial for reaction control and mechanistic studies (model-based design). In addition, special focus was oriented towards green and sustainable reaction conditions. A mixture of water and ethanol was selected as the solvent, which combines a green component and improved miscibility between the water and organic phase. The latter is particularly important to ensure sufficient mass transfer, which could be a limiting factor in such a two-phase reaction. All experiments were carried out at mild reaction condition (room temperature and normal pressure). The residence time of the reaction mixture was initially set to 1 h (flow rate 10 µL/min). The NMR analysis of the eluate (Supplementary Figure S2) shows that the use of the Alg-Cu hydrogel led to a regioselective synthesis of 1,4-disubstituted 1,2,3-triazole with 55% conversion to product. Although the result was encouraging, especially when compared to the related literature protocols (Reddy et al., 2007; Baig and Varma, 2013; Bahsis et al., 2020), there was still room for improvement. Accordingly, the flow rate of the reaction mixture was reduced to 5 µL/min, resulting in a doubling of the residence time. As a result, an excellent conversion to triazole was achieved, namely, 99%. To evaluate the efficiency of the Alg-Cu catalyst, the turnover number (TON) was calculated, considering Cu loading, the molarity of the reagents and the conversion achieved. Note that Cu loading in each hydrogel was estimated based on correlation display in Figure 6, assuming a constant deposition time of 120 min and current density of 3.5 A/m^2. With longer residence time, the TON almost doubled. Due to microfluidic geometry, diffusion in the liquid phase and associated mass transfer limitations can be neglected, which means that diffusion through the gel layer and the kinetics of the catalytic reaction primarily determine the reaction rate. Both mechanisms were evaluated using the mathematical model described in Section 2.7 and discussed in the following paragraphs.

Nonetheless, to put these results into perspective, batch experiments at the same residence time, namely, 2 h, was performed next. For this purpose, Alg-Cu was formed on a cylindrical Cu electrode under the same electrodeposition conditions to ensure comparable Cu loading. The hydrogel-coated electrode was placed in a flask and the reagents were added with a solvent solution. After the same reaction time (2 h), the sample was analysed for the formation of triazole. However, only a conversion of 10% was detected at this elevated reaction time. We assume that the main reason for the observed discrepancy, compared to flow system, was the mass transfer restriction due to batch operation. The results therefore unambiguously confirm the positive effects of the continuous operation, which are emphasised by the process intensification using microfluidic device.

To demonstrate the efficiency of our catalytic system compared to the other catalytic systems reported in the context of CuAAC, the comparative results of copper-catalyzed cycloaddition as a model reaction are summarized in Table 1. The results highlight the efficiency of proposed system, leading to near complete conversion to the desired product with a significantly reduced reaction time and in many cases also with a lower amount of copper required. Consequently, the TON of our system (entry 2) was superior to almost all others, comparable to the Cu(I)-cellulose catalyst and slightly worse than only Cu(II)-poly (hydroxamic acid) catalyst. However, in the case of Cu(I)-cellulose catalyst, copper in the desired Cu (I) oxidation state was utilized, which is somewhat less stable and therefore much less durable and useful. The experiments with Cu(II)-poly (hydroxamic acid) catalyst, on the other hand, require higher temperatures. In addition, both systems resulted in slightly lower conversions. More importantly, however, our system operates in the flow regime, with the microfluidic setup ensuring no or minimal diffusion limitation in the liquid phase under steady-state conditions. Finally, we assume that copper located at or near interfacial surfaces primly participates in the catalytic reaction, which means that the bulk of the copper is intact. This reduces the required amount of Cu and its TON, but also ensures the required strength of the hydrogel, crucial for its stability and reusability.

3.4 Recovery and reusability of the catalyst

For the practical application of such heterogeneous systems, the lifetime of the catalyst and the degree of its reusability are very

TABLE 1 Comparison of the click chemistry of 1,4-disubstituted–1,2,3-triazoles by our protocols with other catalytic methods.

Entry	Catalyst	Cu loading [mol%]	Conditions	Time [h]	Conv. [%]	TON	Ref.
1	Cu(II)-alginate	0.6	H_2O:EtOH 1:1, r.t., flow	1	55	98	This work
2	Cu(II)-alginate	0.6	H_2O:EtOH 1:1, r.t., flow	2	99	190	This work
3	Cu(II)-alginate	0.5	H_2O:EtOH 1:1, r.t., batch	2	10	15	This work
4	Cu(II)-alginate	2.0	H_2O, r.t., batch	24	95	24	Bahsis et al. (2020)
5	Cu(II)-alginate dried	2.0	H_2O, r.t., batch	48	93	23	Bahsis et al. (2020)
6	Cu(II)-alginate	21	H_2O, r.t., batch	18	98	4.6	Reddy et al. (2007)
7	Cu(II)-cellulose	1.2	H_2O, r.t., batch	12	96	40	Bahsis et al. (2018)
8	Cu(I)-cellulose	0.14	H_2O, r.t., batch	4	93	332	Mandal et al., 2017
9	Cu(II)-poly (hydroxamic acid)	0.1	H_2O, 50°C, batch	4	91	910	Mandal et al., 2017
10	Cu(II)-chitosan	n.d.[a]	H_2O, r.t., batch	4	99	~75	Baig and Varma (2013)
11	Cu(II)-polyethylenimine	5	H_2O, r.t., batch	24	98	12	Ben El Ayouchia et al., 2019
12	Cu(II)-PEG-PS[b]	5	H_2O, N_2, r.t., sodium ascorbate (10 mol %), batch	12	97	9.7	Pan et al., 2017

[a]Not determined in mol%, given as CuSO4-chitosan (5 mg).
[b]PEG-PS, poly (ethylene glycol)-polystyrene.

important factors. To address this issue, a series of experiments were performed for the cycloaddition of BA and PA using the recycled Alg-Cu catalyst. All experiments were performed under the same conditions as for entry 2 in Table 1. After completion of the first reaction, the microreactor was washed extensively and stored in a solvent (ethanol-water 50:50) for further use. A fresh reaction mixture was then introduced to microreactor inlet and the reaction protocol was repeated under the same conditions. 5 cycles were performed with the same catalyst without any significant change in its activity. Conversion rates remained consistent over five cycles, demonstrating the catalyst's stability. In addition, the hydrogels were subjected to FT-IR analysis after the fifth cycle and compared with the freshly prepared hydrogel produced by the same process. Apart from a slight decrease in peak intensity in the FT-IR spectra (Supplementary Figure S5), no visible changes were observed, further confirming the recyclability of the catalysts. It is expected that all immobilized copper can participate in the catalytic reaction, i.e., the reaction is not limited to the surface of the hydrogel; rather, the entire gel volume can participate in catalysis. Although this leads to an additional transport limitation (diffusion through the hydrogel layer), it also ensures a high concentration of active sites. Therefore, even if some Cu was diluted from the hydrogel between repeated cycles, this did not affect the catalytic activity. Nonetheless, Cu leaching was determined by AAS analysis of the catalyst before and after the fifth reaction cycle. The Cu concentration decreased slightly, from 0.56% to 0.49% before and after the reaction. Although some decrease was observed, the leaching of Cu was very moderate. Interestingly, no Cu was detected in the eluate flow after completion of the reaction, indicating that its concentration was below the detection limit. Subsequently, the SEM image of the catalyst obtained after the fifth reaction cycle was analysed. No significant change in the Alg-Cu morphology was observed (Figure 5B), indicating the retention of the intrinsic porous structure after recycling, which is vital for the preservation of catalytic activity. It should be noted, however, that the pore size and morphology of the hydrogel observed in the SEM may not fully reflect its structure in the reaction mixture. Finally, the high catalytic activity, ease of preparation and modification, and notable recyclability of the Alg-Cu hydrogel make this catalyst an excellent candidate for various environmental applications.

The proposed system, based on Alg-Cu catalysts immobilized in microfluidic systems, thus represents a significant advance in the synthesis of fine chemicals through green chemistry. By employing Cu-alginate hydrogels as the copper source for catalysis in microfluidic flow-through systems, this approach leverages the benefits of microfluidics to increase productivity and process intensification. In particular, microfluidic systems enable controlled, continuous flow regimes that ensure consistent reaction conditions, leading to higher productivity and efficiency in chemical synthesis. The microfluidic environment enhances reaction kinetics and mass transfer, which are critical for rapid and efficient chemical reactions. In addition, the unique properties of alginate, a natural biopolymer, facilitate the immobilization of copper ions, which enhances catalytic activity while adhering to the principles of sustainable chemistry through the use of renewable resources. The ability to precisely control the formation of the hydrogel by electrodeposition in microchannels enables tailored catalytic properties and optimizes both the chemical reaction process and the reusability of the catalyst. This innovative integration not only streamlines the synthesis process, but also minimizes waste and energy consumption, compared to the use

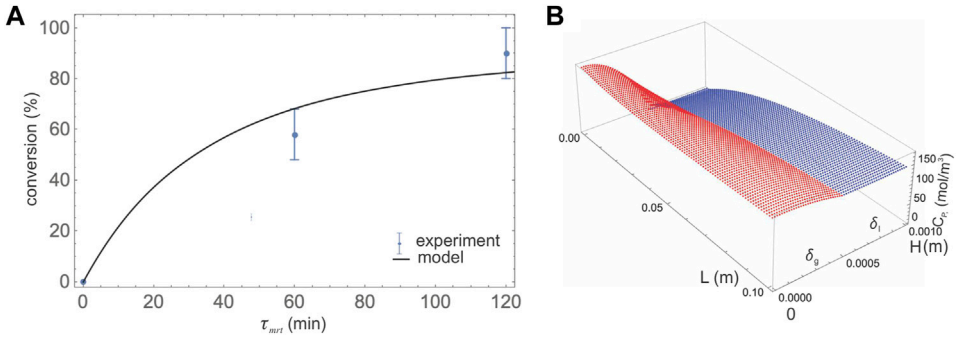

FIGURE 8
The evaluation of conversion as a function of residence time at kinetic constant set to $0.49 \cdot 10^{-5}$ [m^3 mol^{-1} s^{-1}] **(A)**. The concentration distribution in gel phase (red) and liquid phase (blue) at residence time 60 min **(B)**.

of free copper salts, representing a substantial step towards more sustainable and efficient chemical production.

3.5 Model based simulations

Finally, the model-based design described in detail in section 2.7 was used to predict reaction kinetics and transport phenomena. The model assumes convective and diffusion mass transfer, diffusion through the gel layer and a second-order catalytic reaction, with kinetic constants derived from variable experimental conditions. The model enables the integration and evaluation of various complex behaviors in microfluidic systems and provides a theoretical framework for understanding and optimizing catalytic reactions in the design of sustainable chemical processes. Such a model-based design facilitates the development of complex heterogeneous reactions and provides a mechanistic approach to system optimization and control.

Since only limited experimental data was obtained for our system so far, some of the required parameters were determined as fitting parameters. Based on the reaction mechanism (Figure 7), a second order catalytic reaction was assumed and the value of the reaction kinetic constant was fitted to the experimental data. Based on the best fit, the kinetic constant was set to $0.49 \cdot 10^{-5}$ [m^3 mol^{-1} s^{-1}]. Furthermore, the diffusion coefficient in the liquid phase was estimated based on the Scheibel and Wilke-Chang correlations (Milozic et al., 2014), while the diffusion coefficient in the gel phase was assumed to be 10 times lower (typically applied estimate (Menegatti et al., 2024)). As shown in Figure 8, the model predicts how the conversion of substrates to products is affected by the residence time, which is adjusted by the flow rate of the reaction mixture. As expected, the longer the residence time, the higher the conversion. Although the predictions agree with the experimental data, some discrepancy in the exact values was observed. It should be noted that these predictions are only preliminary and further investigations will be conducted in the following phases of our research. Accordingly, batch experiments will be performed to empirically determine the true kinetic parameters. In addition, the effective diffusion in the gel layer will be determined experimentally using a custom-built cell with two tanks and a simplified and linearized derivation of Fick's second law for the diffusion calculation (Menegatti et al., 2024). This will allow us to refine our model with actual data, enhancing its predictive accuracy and reliability.

Although the model validation still requires some fine-tuning, the simulated concentration profiles deliver the expected concentration profiles. Namely, distinct concentration gradient across the thickness of the gel can be seen, while the gradient along the width of the channel for the liquid phase is much smaller and almost negligible. The difference in the diffusion coefficient in both phases is the main reason for the observed differences. In addition to the diffusion into the gel layer, the conversion is naturally also influenced by the kinetics of the chemical reaction. To improve diffusion and reaction efficiency in the hydrogel, we can optimize the electrodeposition conditions to increase porosity, modify the composition of the hydrogel with biopolymers or crosslinkers for a more open structure, and increase the flow rate of reactants to maintain higher concentration gradients. Time-scale analysis (TSA) is an innovative analytical tool that defines the relevant process windows, reveals the limiting phenomena (such as catalytic reaction, mass transfer) and guides optimization (Jovanovic et al., 2021a; 2021b). It is an engineering analytical tool and design approach in which all processes, rates, fluxes, contact times or other dynamic phenomena in the system are represented by their own characteristic time, which adequately represents the rate/intensity of each dynamic phenomenon in a chemical process. Moreover, the characteristic times are controlled by users to enable meaningful analysis of chemical processes and provide insights or suggestions for successful design decisions. The initial results of the TSA analysis indicate comparable effects of the two main mechanisms, i.e., gel diffusion and reaction kinetics, on the conversion rate. However, a more detailed analysis will be performed once further experiments are conducted, allowing the determination of the optimal hydrogel thickness for an optimal turnover number (TON).

4 Conclusion

This study has demonstrated the significant potential of copper-alginate catalysts in enhancing the efficiency of 1,3-dipolar cycloaddition reactions and other oxidative transformations. The

integration of these catalysts into microfluidic systems provides a sustainable and scalable strategy that enables precise control over reaction conditions, including rapid transport phenomena and optimized reaction kinetics. The microfluidic platform, combined with stimuli-responsive materials such as copper-alginate hydrogels, enables precise electrodeposition and tuning of catalytic properties by adjusting copper content and gel morphology. The characterization and optimization of Cu-alginate hydrogels and their successful use in green catalysis demonstrate the potential for the development of environmentally friendly methods for organic synthesis. In addition, the reusability of the catalyst underscores the practical applicability of this system, aligning with the principles of sustainable chemistry.

This approach not only opens up new pathways for the application of biopolymer-supported catalysts in organic synthesis, but also exemplifies the value of microfluidic devices in enhancing chemical process sustainability and efficiency. The results suggest that copper-alginate catalysts in the context of microfluidic technology represent a promising avenue for future research in green chemistry and process intensification. Finally, the use of advanced computational tools such as time scale analysis, CFD analysis and mathematical modeling, further underscored the benefits of model-based design. These tools allow for in-depth simulations of fluid dynamics and reaction mechanisms, providing insights that guide the optimization of catalyst performance and microfluidic design. By leveraging such models, researchers can predict the behavior of the catalytic system under different conditions, enhancing process efficiency and minimizing trial-and-error testing.

Data availability statement

The original contributions presented in the study are included in the article/Supplementary Material, further inquiries can be directed to the corresponding author.

Author contributions

AR: Writing–review and editing, Formal Analysis, Investigation. MG: Formal Analysis, Investigation, Data curation, Methodology, Writing–review and editing. IP: Data curation, Methodology, Writing–review and editing, Funding acquisition, Project administration, Software. RA: Data curation, Methodology, Project administration, Software, Writing–review and editing, Conceptualization, Writing–original draft.

Funding

The author(s) declare that financial support was received for the research, authorship, and/or publication of this article. The author(s) declare that financial support was received for the research, authorship, and/or publication of this article. This work has benefitted from the support of the following projects, which are gratefully acknowledged: Slovenian Research Agency (research core funding No. P2-0191 and project L2-3161 (B)), the Ministry of Higher Education, Science and Innovation (Grant No. 9147) and EU Horizon 2020 M.ERA.net (Grant No. 958174).

Acknowledgments

The authors acknowledge the financial support from the Slovenian Research Agency and from the Ministry of Higher Education, Science and Innovation.

Conflict of interest

The authors declare that the research was conducted in the absence of any commercial or financial relationships that could be construed as a potential conflict of interest.

Publisher's note

Supplementary material

The Supplementary Material for this article can be found online at: https://www.frontiersin.org/articles/10.3389/fceng.2024.1434131/full#supplementary-material

References

Aflak, N., Ben El Ayouchia, H., Bahsis, L., Anane, H., Julve, M., and Stiriba, S. E. (2022). Recent advances in copper-based solid heterogeneous catalysts for azide-alkyne cycloaddition reactions. *Int. J. Mol. Sci.* 23 (4), 2383. doi:10.3390/ijms23042383

Alonso, F., Moglie, Y., Radivoy, G., and Yus, M. (2010). Unsupported copper nanoparticles in the 1,3-dipolar cycloaddition of terminal alkynes and azides. *Eur. J. Org. Chem.* 2010 (10), 1875–1884. doi:10.1002/ejoc.200901446

Ambrozic, R., Krühne, U., and Plazl, I. (2024). Microfluidics with redox-responsive hydrogels for on-demand BPA degradation. *Chem. Eng. J.* 485, 149542. doi:10.1016/j.cej.2024.149542

Ambrozic, R., and Plazl, I. (2021). Development of an electrically responsive hydrogel for programmable *in situ* immobilization within a microfluidic device. *Soft Matter* 17 (28), 6751–6764. doi:10.1039/d1sm00510c

Bahsis, L., Ablouh, E., Anane, H., Taourirte, M., Julve, M., and Stiriba, S. E. (2020). Cu(ii)-alginate-based superporous hydrogel catalyst for click chemistry azide-alkyne cycloaddition type reactions in water. *Rsc Adv.* 10 (54), 32821–32832. doi:10.1039/d0ra06410f

Bahsis, L., Ben El Ayouchia, H., Anane, H., Benhamou, K., Kaddami, H., Julve, M., et al. (2018). Cellulose copper as bio-supported recyclable catalyst for the clickable azide-alkyne 3+2 cycloaddition reaction in water. *Int. J. Biol. Macromol.* 119, 849–856. doi:10.1016/j.ijbiomac.2018.07.200

Baig, R. B. N., and Varma, R. S. (2013). Copper on chitosan: a recyclable heterogeneous catalyst for azide-alkyne cycloaddition reactions in water. *Green Chem.* 15 (7), 1839–1843. doi:10.1039/c3gc40401c

Balakrishnan, A., Chinthala, M., and Polagani, R. K. (2024). 3D kaolinite/g-C3N4-alginate beads as an affordable and sustainable photocatalyst for wastewater remediation. *Carbohydr. Polym.* 323, 121420. doi:10.1016/j.carbpol.2023.121420

Ben El Ayouchia, H., ElMouli, H., Bahsis, L., Anane, H., Laamari, R., Gómez-García, C. J., et al. (2019). Hyperbranched polyethylenimine-supported copper(II) ions as a macroliganted homogenous catalyst for strict click reactions of azides and alkynes in water. *J. Organomet. Chem.* 898, 120881. doi:10.1016/j.jorganchem.2019.120881

De, S., Dokania, A., Ramirez, A., and Gascon, J. (2020). Advances in the design of heterogeneous catalysts and thermocatalytic processes for CO_2 utilization. *Acs Catal.* 10 (23), 14147–14185. doi:10.1021/acscatal.0c04273

Dhital, R. N., Karnonsatikul, C., Somsook, E., Bobuatong, K., Ehara, M., Karanjit, S., et al. (2012). Low-temperature carbon-chlorine bond activation by bimetallic gold/palladium alloy nanoclusters: an application to ullmann coupling. *J. Am. Chem. Soc.* 134 (50), 20250–20253. doi:10.1021/ja309606k

Dohendou, M., Pakzad, K., Nezafat, Z., Nasrollahzadeh, M., and Dekamin, M. G. (2021). Progresses in chitin, chitosan, starch, cellulose, pectin, alginate, gelatin and gum based (nano)catalysts for the Heck coupling reactions: a review. *Int. J. Biol. Macromol.* 192, 771–819. doi:10.1016/j.ijbiomac.2021.09.162

Dong, Y. C., Dong, W. J., Cao, Y. N., Han, Z. B., and Ding, Z. Z. (2011). Preparation and catalytic activity of Fe alginate gel beads for oxidative degradation of azo dyes under visible light irradiation. *Catal. Today* 175 (1), 346–355. doi:10.1016/j.cattod.2011.03.035

El Kadib, A. (2015). Chitosan as a sustainable organocatalyst: a concise overview. *Chemsuschem* 8 (2), 217–244. doi:10.1002/cssc.201402718

Fraczyk, J., Wasko, J., Walczak, M., Kaminski, Z. J., Puchowicz, D., Kaminska, I., et al. (2020). Conjugates of copper alginate with arginine-glycine-aspartic acid (RGD) for potential use in regenerative medicine. *Materials* 13 (2), 337. doi:10.3390/ma13020337

Ghosh, D., Dhibar, S., Dey, A., Manna, P., Mahata, P., and Dey, B. (2020). A Cu(II)-Inorganic Co-crystal as a versatile catalyst towards 'click' chemistry for synthesis of 1,2,3-triazoles and β-hydroxy-1,2,3-triazoles. *Chemistryselect* 5 (1), 75–82. doi:10.1002/slct.201904225

Goy, C. B., Chaile, R. E., and Madrid, R. E. (2019). Microfluidics and hydrogel: a powerful combination. *React. Funct. Polym.* 145, 104314. doi:10.1016/j.reactfunctpolym.2019.104314

Huang, Y. H., Jazani, A. M., Howell, E. P., Oh, J. K., and Moffitt, M. G. (2020). Controlled microfluidic synthesis of biological stimuli-responsive polymer nanoparticles. *Acs Appl. Mater. Interfaces* 12 (1), 177–190. doi:10.1021/acsami.9b17101

Jiménez-González, C., Poechlauer, P., Broxterman, Q. B., Yang, B. S., Ende, D. A., Baird, J., et al. (2011). Key green engineering research areas for sustainable manufacturing: a perspective from pharmaceutical and fine chemicals manufacturers. *Org. Process Res. Dev.* 15 (4), 900–911. doi:10.1021/op100327d

Jovanovic, G. N., Coblyn, M. Y., and Plazl, I. (2021a). Time scale analysis & characteristic times in microscale-based bio-chemical processes: Part II - bioreactors with immobilized cells, and process flowsheet analysis. *Chem. Eng. Sci.* 236, 116499. doi:10.1016/j.ces.2021.116499

Jovanovic, G. N., Coblyn, M. Y., and Plazl, I. (2021b). Time scale analysis & characteristic times in microscale-based chemical and biochemical processes: Part I - concepts and origins. *Chem. Eng. Sci.* 238, 116502. doi:10.1016/j.ces.2021.116502

Kang, D. H., Kim, S. M., Lee, B., Yoon, H., and Suh, K. Y. (2013). Stimuli-responsive hydrogel patterns for smart microfluidics and microarrays. *Analyst* 138 (21), 6230–6242. doi:10.1039/c3an01119d

Mandal, B. H., Rahman, M. L., Yusoff, M. M., Chong, K. F., and Sarkar, S. M. (2017). Bio-waste corn-cob cellulose supported poly (hydroxamic acid) copper complex for Huisgen reaction: Waste to wealth approach. *Carbohydr. Polym.* 156, 175–181. doi:10.1016/j.carbpol.2016.09.021

Masuda, K., Ichitsuka, T., Koumura, N., Sato, K., and Kobayashi, S. (2018). Flow fine synthesis with heterogeneous catalysts. *Tetrahedron* 74 (15), 1705–1730. doi:10.1016/j.tet.2018.02.006

Menegatti, T., Plazl, I., and Znidarsic-Plazl, P. (2024). Model-based design of continuous biotransformation in a microscale bioreactor with yeast cells immobilized in a hydrogel film. *Chem. Eng. J.* 483, 149317. doi:10.1016/j.cej.2024.149317

Milozic, N., Lubej, M., Novak, U., Znidarsic-Plazl, P., and Plazr, I. (2014). Evaluation of diffusion coefficient determination using a microfluidic device. *Chem. Biochem. Eng. Q.* 28 (2), 215–223. doi:10.15255/cabeq.2014.1938

Milozic, N., Stojkovic, G., Vogel, A., Bouwes, D., and Znidarsic-Plazl, P. (2018). Development of microreactors with surface-immobilized biocatalysts for continuous transamination. *New Biotechnol.* 47, 18–24. doi:10.1016/j.nbt.2018.05.004

Newman, S. G., and Jensen, K. F. (2013). The role of flow in green chemistry and engineering. *Green Chem.* 15 (6), 1456–1472. doi:10.1039/c3gc40374b

Nie, J., Gao, Q., Wang, Y. D., Zeng, J. H., Zhao, H. M., Sun, Y., et al. (2018). Vessel-on-a-chip with hydrogel-based microfluidics. *Small* 14 (45), e1802368. doi:10.1002/smll.201802368

Pan, S., Yan, S., Osako, T., and Uozumi, Y. (2017). Batch and Continuous-Flow Huisgen 1,3-Dipolar Cycloadditions with an Amphiphilic Resin-Supported Triazine-Based Polyethyleneamine Dendrimer Copper Catalyst. *ACS Sustainable Chem. Eng.* 5, 10722–10734. doi:10.1021/acssuschemeng.7b02646

Pohar, A., Znidarsic-Plazl, P., and Plazl, I. (2012). Integrated system of a microbioreactor and a miniaturized continuous separator for enzyme catalyzed reactions. *Chem. Eng. J.* 189, 376–382. doi:10.1016/j.cej.2012.02.035

Reddy, K. R., Rajgopal, K., and Kantam, M. L. (2007). Copper-alginates: a biopolymer supported Cu(II) catalyst for 1,3-dipolar cycloaddition of alkynes with azides and oxidative coupling of 2-naphthols and phenols in water. *Catal. Lett.* 114 (1-2), 36–40. doi:10.1007/s10562-007-9032-x

Roquero, D. M., Othman, A., Melman, A., and Katz, E. (2022). Iron(iii)-cross-linked alginate hydrogels: a critical review. *Mater. Adv.* 3 (4), 1849–1873. doi:10.1039/d1ma00959a

Shiri, P., and Aboonajmi, J. (2020). A systematic review on silica-carbon-and magnetic materials-supported copper species as efficient heterogeneous nanocatalysts in "click" reactions. *Beilstein J. Org. Chem.* 16, 551–586. doi:10.3762/bjoc.16.52

Sun, K. K., Shan, H. B., Lu, G. P., Cai, C., and Beller, M. (2021). Synthesis of *N*-heterocycles via oxidant-free dehydrocyclization of alcohols using heterogeneous catalysts. *Angew. Chemie-International Ed.* 60 (48), 25188–25202. doi:10.1002/anie.202104979

Tamborini, L., Fernandes, P., Paradisi, F., and Molinari, F. (2018). Flow bioreactors as complementary tools for biocatalytic process intensification. *Trends Biotechnol.* 36 (1), 73–88. doi:10.1016/j.tibtech.2017.09.005

Vicente, F. A., Plazl, I., Ventura, S. P. M., and Znidarsic-Plazl, P. (2020). Separation and purification of biomacromolecules based on microfluidics. *Green Chem.* 22 (14), 4391–4410. doi:10.1039/c9gc04362d

Wang, B. B., Ran, M., Fang, G. G., Wu, T., Tian, Q. W., Zheng, L. Q., et al. (2020). Palladium nano-catalyst supported on cationic nanocellulose-alginate hydrogel for effective catalytic reactions. *Cellulose* 27 (12), 6995–7008. doi:10.1007/s10570-020-03127-4

Wohlgemuth, R., Plazl, I., Znidarsic-Plazl, P., Gernaey, K. V., and Woodley, J. M. (2015). Microscale technology and biocatalytic processes: opportunities and challenges for synthesis. *Trends Biotechnol.* 33 (5), 302–314. doi:10.1016/j.tibtech.2015.02.010

Wu, J. Z., and Kozlowski, M. C. (2022). Catalytic oxidative coupling of phenols and related compounds. *Acs Catal.* 12 (11), 6532–6549. doi:10.1021/acscatal.2c00318

Xia, M., Kang, S. M., Lee, G. W., Huh, Y. S., and Park, B. J. (2019). The recyclability of alginate hydrogel particles used as a palladium catalyst support. *J. Industrial Eng. Chem.* 73, 306–315. doi:10.1016/j.jiec.2019.01.042

Zhang, H. Q., Riomet, M., Roller, A., and Maulide, N. (2020). Synthesis of novel heterocycles by amide activation and umpolung cyclization. *Org. Lett.* 22 (6), 2376–2380. doi:10.1021/acs.orglett.0c00571

Zhang, J. M., Han, D. H., Zhang, H. J., Chaker, M., Zhao, Y., and Ma, D. L. (2012). *In situ* recyclable gold nanoparticles using CO_2-switchable polymers for catalytic reduction of 4-nitrophenol. *Chem. Commun.* 48 (94), 11510–11512. doi:10.1039/c2cc35784d